Electronic supporting information for

Fluoranthene based derivatives for multimodal anti-counterfeiting and detection of nitroaromatics

Kasthuri Selvaraj,[a] Prasanth Palanaisamy,[a] Marimuthu Manikandan,[b] Praveen B. Managutti,[c] Palanivelu Sangeetha,[b] Sharmarke Mohamed,[c] Rajesh Pamanji[d], Joseph Selvind, Sohrab Nasiri,[e,f] , Stepan Kment [f,g] and Venkatramaiah Nutalapati*[a]

[a]Department of Chemistry, Faculty of Engineering and Technology, SRM Institute of Science and Technology (SRMIST), Kattankulathur-603203, India.

[b]Department of Chemistry, School of Advanced Sciences, Vellore Institute of Technology Chennai Campus, Chennai - 600 127, Tamilnadu, India

[c]*Chemical Crystallography Laboratory, Khalifa University of Science and Technology, Abu Dhabi, PO BOX 127788, United Arab Emirates.*

[d]*Department of Microbiology, Pondicherry University, Puducherry 605014, India.*

[e] *Faculty of Mechanical Engineering, Optical Measurement Laboratory, Kaunas University of Technology, Studentu Street 56, L-116, Kaunas, LT 51373, Lithuania*

[f] *CEET, Nanotechnology Centre, VŠB-Technical University of Ostrava, 17. Listopadu 2172/15, Ostrava-Poruba 708 00, Czech Republic*

[g] *Czech Advanced Technology and Research Institute, Regional Centre of Advanced Technologies and Materials Department, Palacký University Olomouc, Šlechtitelů 27, Olomouc 78371, Czech Republic.*

To whom correspondence should be addressed

Dr. Venkatramaiah Nutalapati, E-mail: *nvenkat83@gmail.com/venkatrv1@srmist.edu.in*

Contents

1. Synthesis

1.1. Synthesis of 7,9-diphenyl-8H-cyclopenta[a]acenaphthylen-8-one (3)

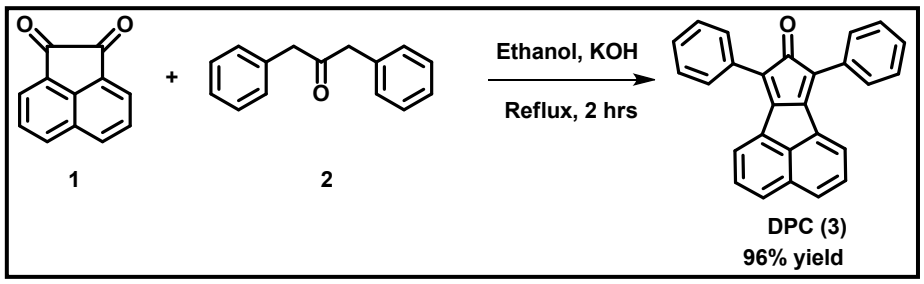

Scheme S1 Synthesis of 7,9-diphenyl-8H-cyclopenta[a]acenaphthylen-8-one, (**3**)

A two-necked 250 mL round bottom flask was placed with a reflux condenser and rubber septum and charged with diphenylacetone (5.75 g, 27.5 mmol) and acenenapthenequinone (5.00 g, 27.5 mmol). 70 ml of Ethanol was added and the mixture was brought to reflux condition, at which point 2.5 mL of ethanolic potassium hydroxide was added drop by drop. The reaction immediately turns violent followed by black precipitate formed. After 15 minutes the reaction vessel was capped and cooled to 0 °C. The pure compound 3 (9.10 g, 92% yield) was then collected by filtration as a deep purple crystalline solid.[1] ^{1}H NMR (500 MHz, $CDCl_3$): δ 8.07 (d, J = 7.2 Hz, 2H), 7.87 (d, J = 8.2 Hz, 2H), 7.83 (dd, J = 8.2, 1.2 Hz, 4H), 7.59 (dd, J = 8.2, 7.2 Hz, 2H), 7.52 (dd, J = 10.9, 4.5 Hz, 4H), 7.42 (d, J = 7.4 Hz, 2H). HR-MS: calculated: 356.1201 found: 357.1278 $[M+1]^+$.

2. Characterization of 3

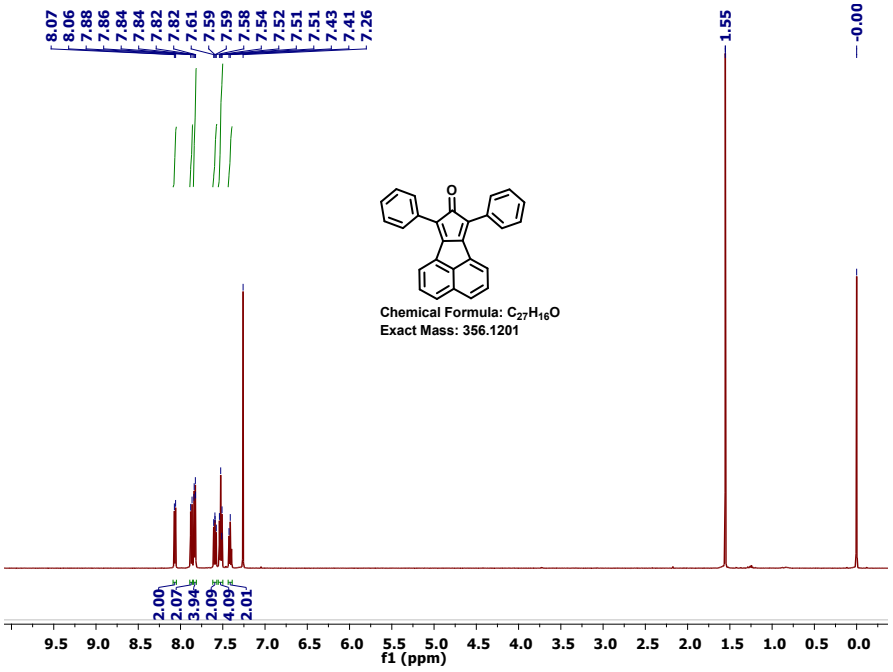

Fig. S1 ^{1}H NMR (500 MHz) spectrum of compound **3** in $CDCl_3$.

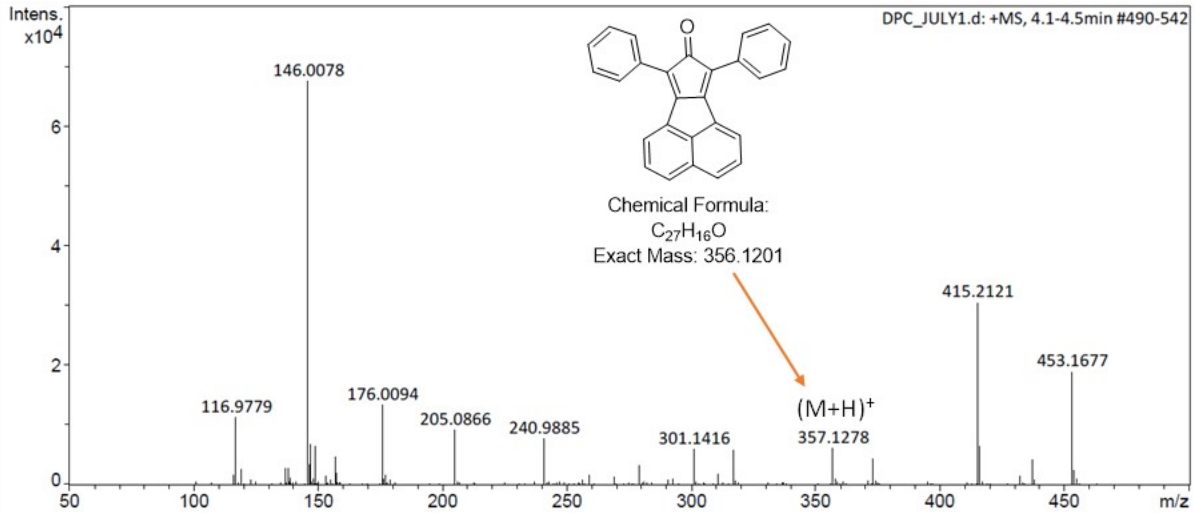

Fig. S2 HR-MS spectrum of compound 3.

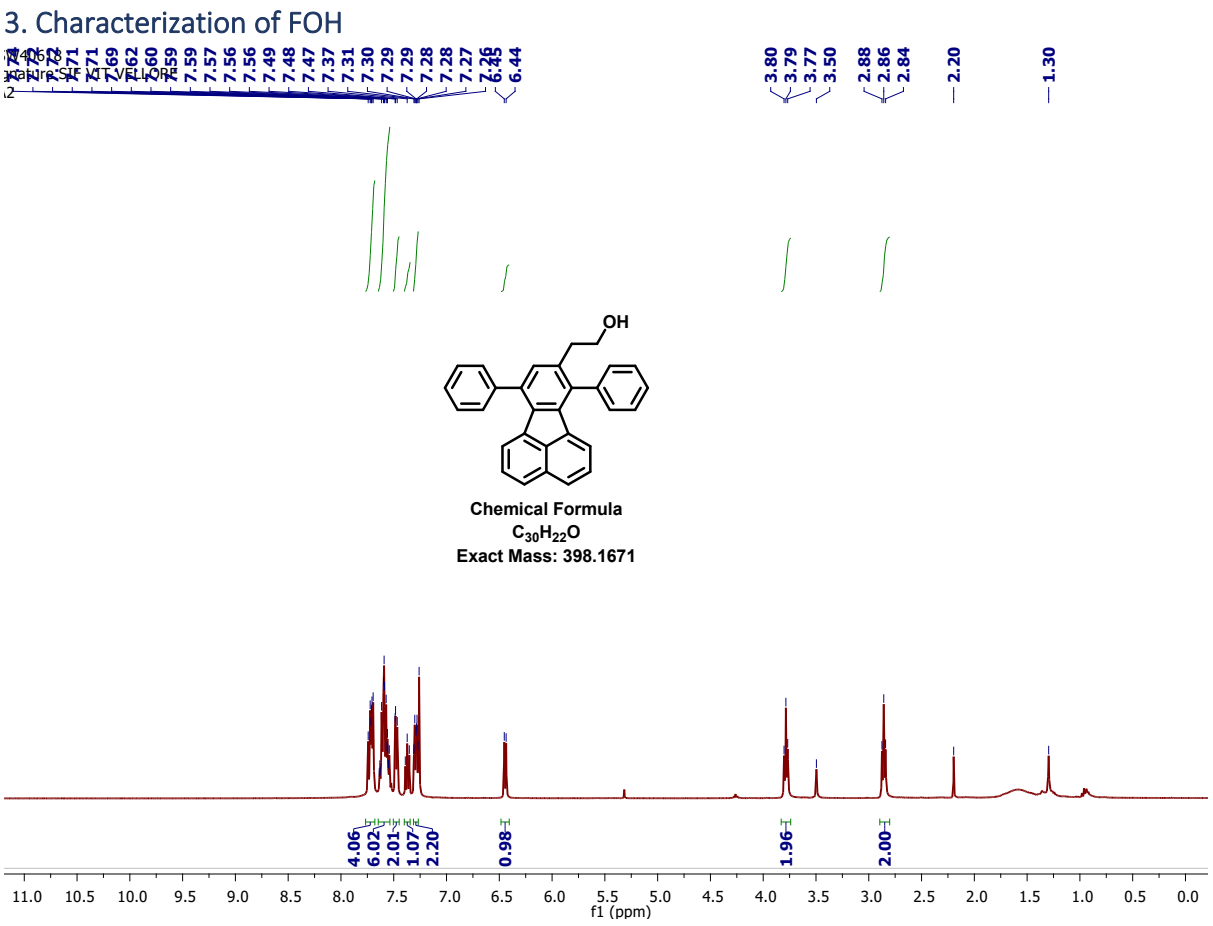

Fig. S3 ^{1}H NMR (400 MHz) spectrum of compound FOH in $CDCl_3$.

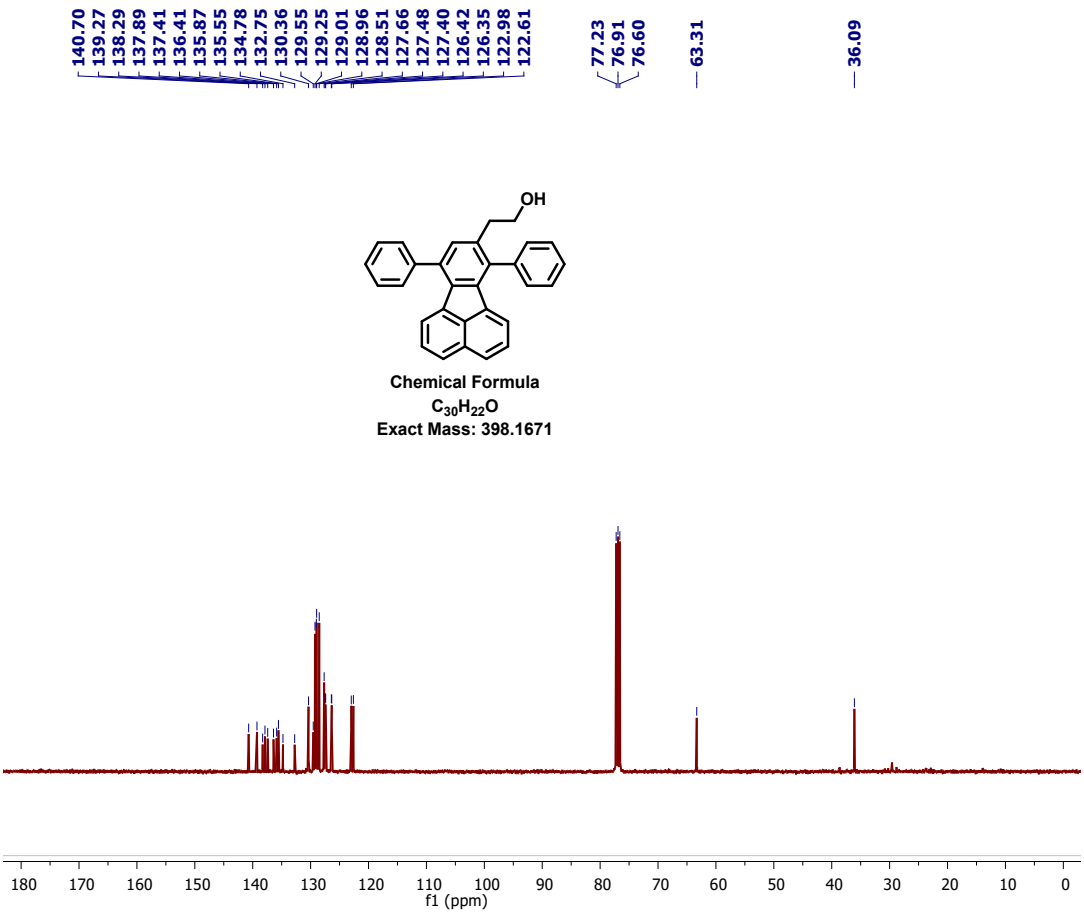

Fig. S4 ^{13}C NMR (100 MHz) spectrum of compound FOH in $CDCl_3$.

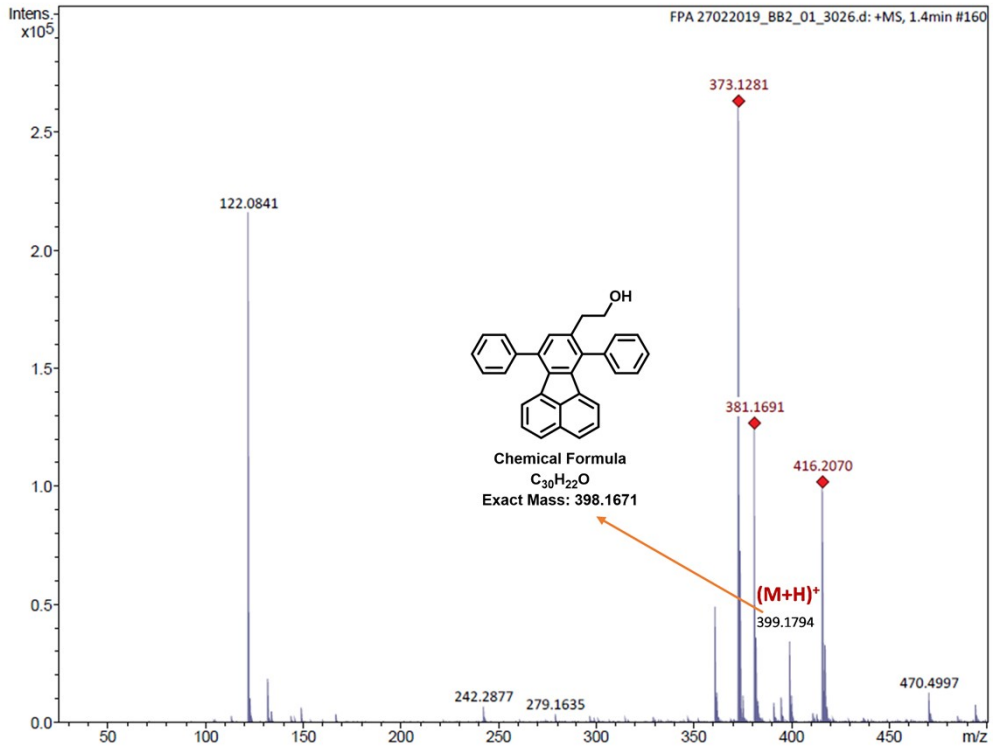

Fig. S5 HR-MS spectrum of compound FOH.

4. Characterization of FSH

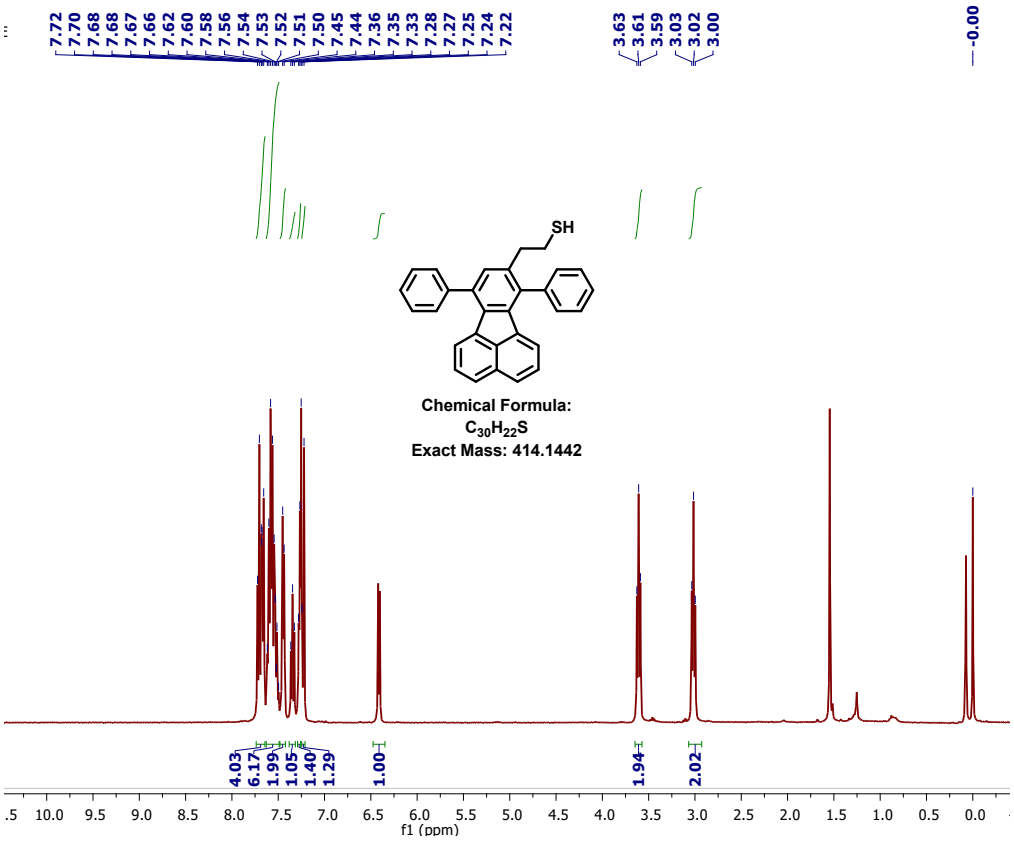

Fig. S6 ^{1}H NMR (400 MHz) spectrum of compound FSH in $CDCl_3$.

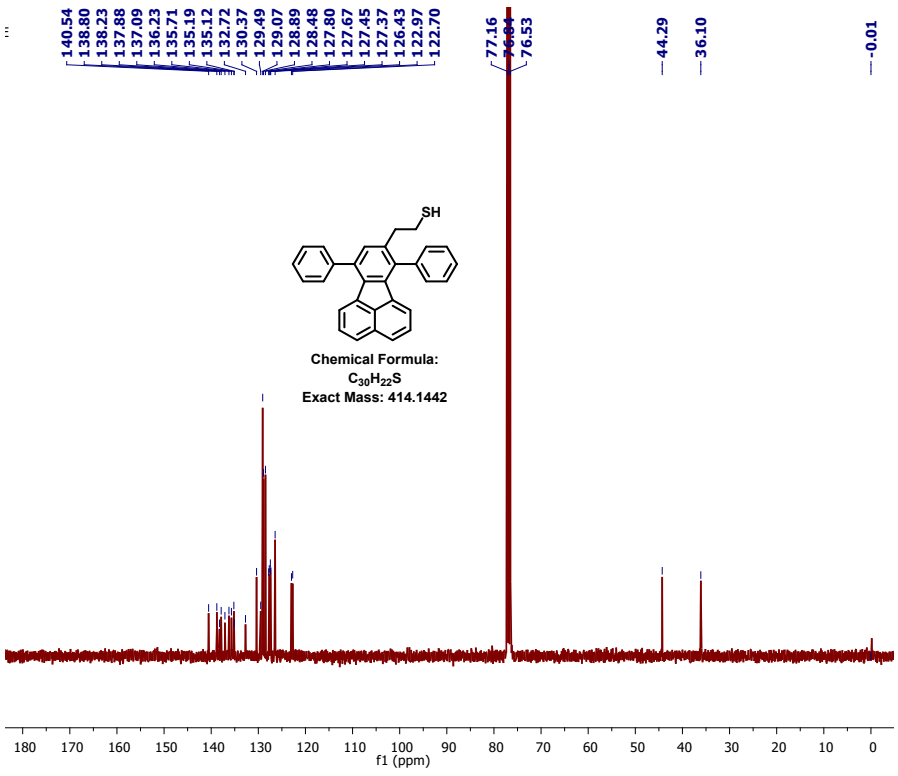

Fig. S7 ^{13}C NMR (100 MHz) spectrum of compound FSH in $CDCl_3$.

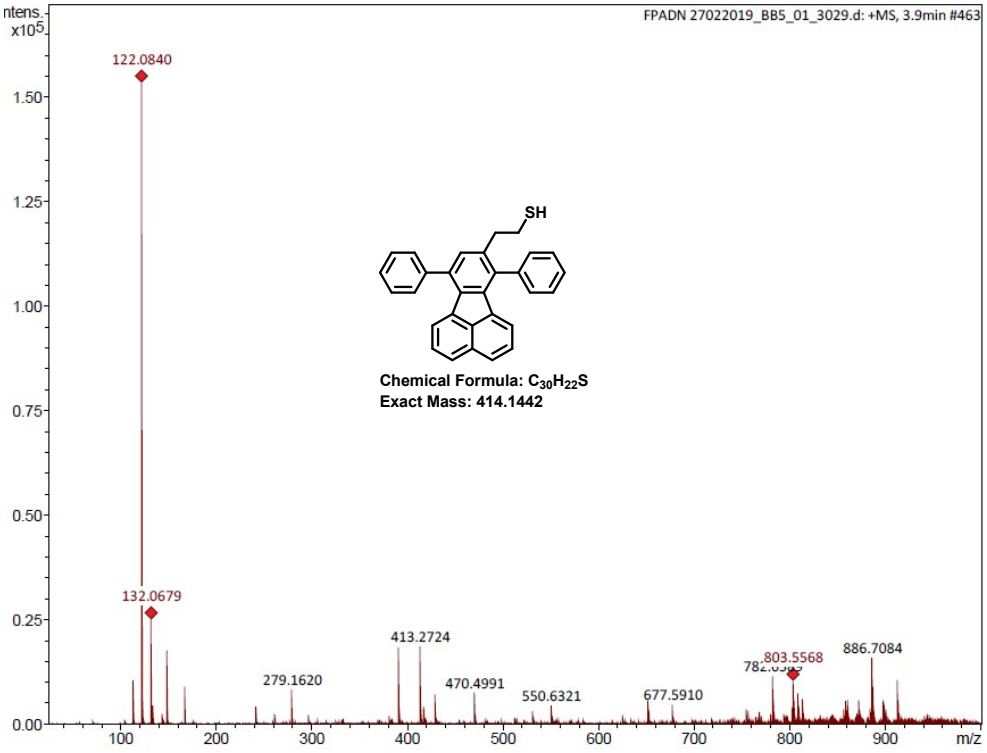

Fig. S8 HR-MS spectrum of compound FSH.

5. Mechanism of FSH from FOH

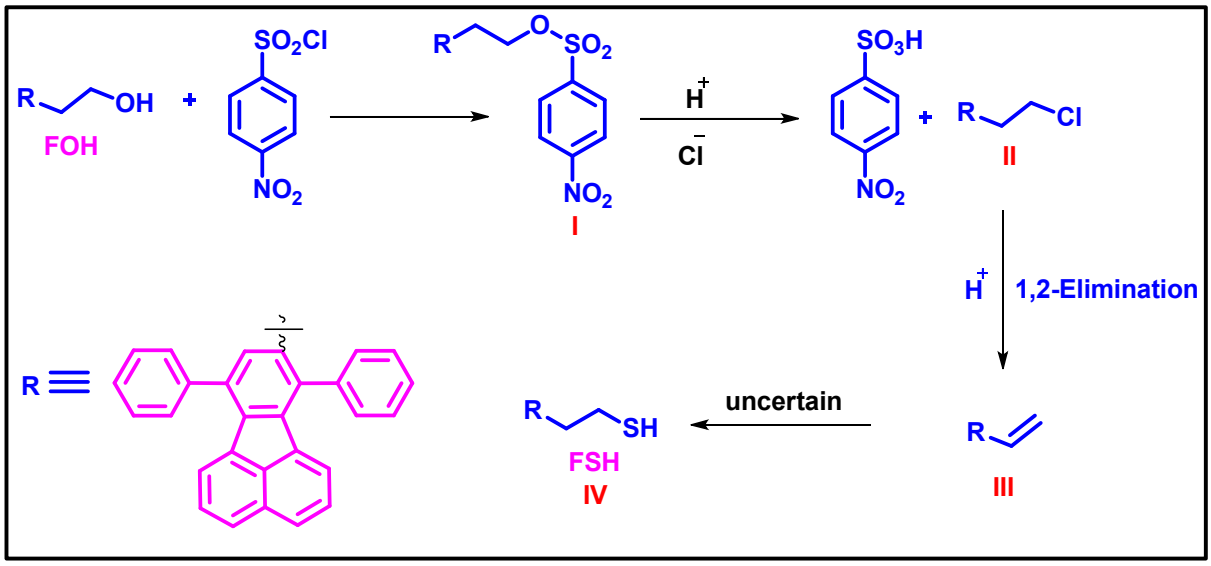

Fig. S9 The proposed mechanism from FOH to FSH transformation.

6. Synthesis of 2-(7,10-diphenylfluoranthen-8-yl)ethanethiol.1,3-dinitrobenzene (FSH-adduct)

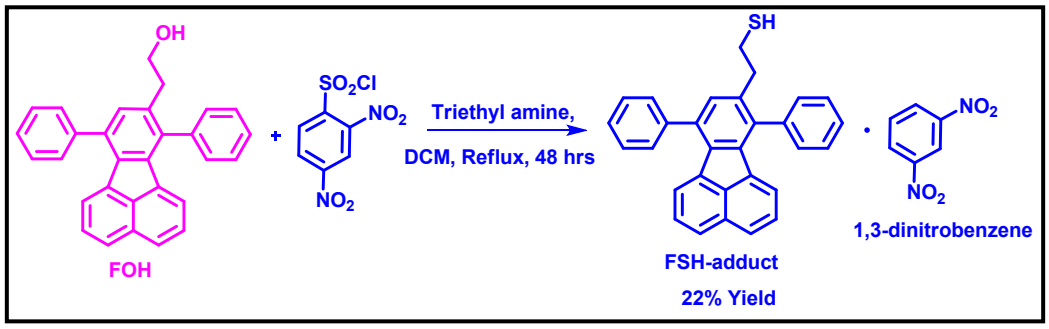

Scheme S2. Synthesis of 2-(7,10-diphenylfluoranthen-8-yl)ethanethiol.1,3-dinitrobenzene FSH-adduct.

In 25 mL round bottom flask, FOH (250 mg, 0.628 mmol) was taken and dissolved in 5 mL of CH_2Cl_2 under nitrogen atmosphere. To this solution, 2,4-dinitrobenzenesulfonyl chloride (837 mg, 3.14 mmol, 5 equiv) in 5 mL of CH_2Cl_2 and triethylamine (3 mL) in 30 mL of CH_2Cl_2 was added dropwise at 0 ^oC for 30 min. The reaction mixture was broguth to room temperature and carried out for 12 h under a nitrogen environment, during that time the mixture colour changed from pale yellow-orange to intense yellow-orange. Further, the temperature of reaction mixture was brought to 40 ^oC for 48 hrs. Afterwards, the reaction mixture was cooled to room temperature and washed with 1N HCl and brine solution. The solvents were dried over anhydrous Na_2SO_4, filtered, and evaporated under vacuum. The reaction mixture was recrystallized with different solvents to remove the impurities. After recrystallization of the crude, left allowed to grow the crystals, which were collected and utilised for further characterization. The crystals were collected and recorded the ^1H and ^{13}C NMR and Mass to confirm the product FSH-adduct. The result was a yellow solid (22% yield). ^1H NMR (400 MHz, $CDCl_3$) δ 7.74 – 7.65 (m, 4H), 7.64 – 7.49 (m, 6H), 7.47 – 7.42 (m, 2H), 7.35 (t, J = 7.6 Hz, 1H), 7.26 (td, J = 10.8, 7.5 Hz, 4H), 6.42 (d, J = 7.1 Hz, 1H), 3.61 (t, J = 7.7 Hz, 2H), 3.02 (t, J = 7.7 Hz, 2H). ^{13}C NMR (100 MHz, $CDCl_3$) δ 140.88, 139.13, 138.55, 138.21, 137.41, 136.56, 136.04, 135.52, 135.45, 133.05, 130.69, 129.82, 129.39, 129.21, 128.80, 128.12, 127.99, 127.76, 127.69, 126.75, 123.29, 123.02, 77.48, 77.16, 76.84, 44.60, 36.42, 29.85. ESI-MS: 581.2500 $[M-1]^+$.

7. Characterization of FSH-adduct

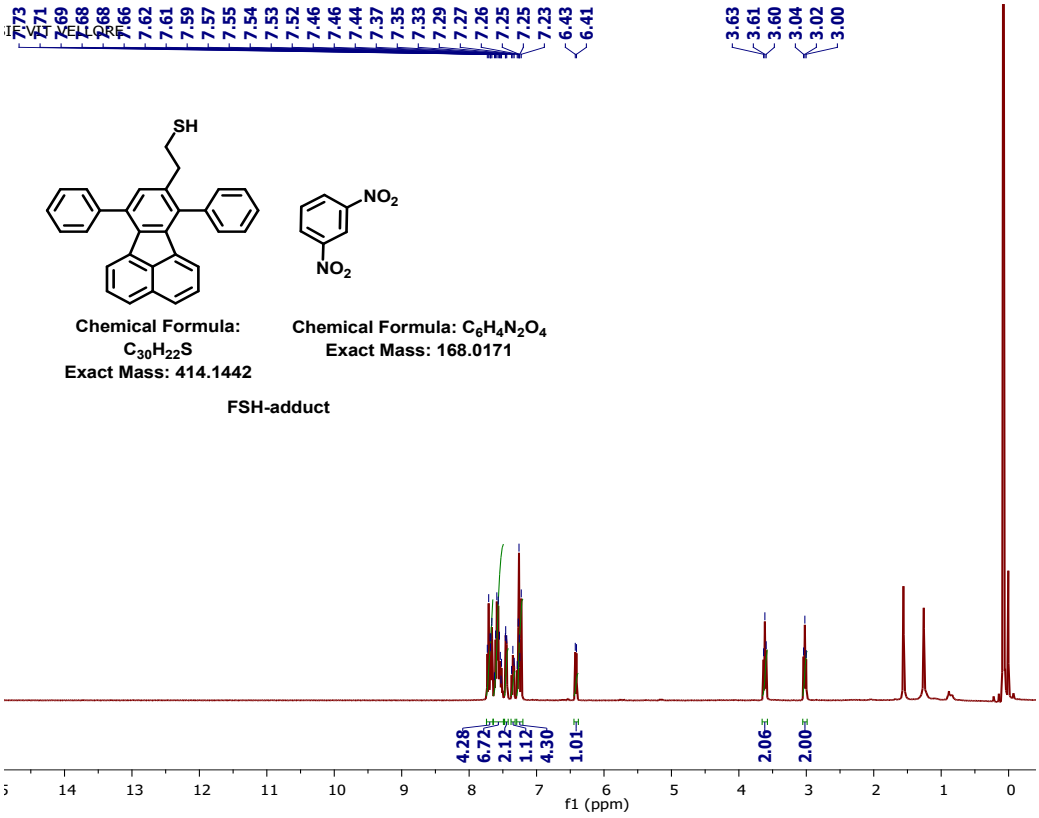

Fig. S10 ^{1}H NMR (400 MHz) spectrum of compound FSH-adduct in $CDCl_3$.

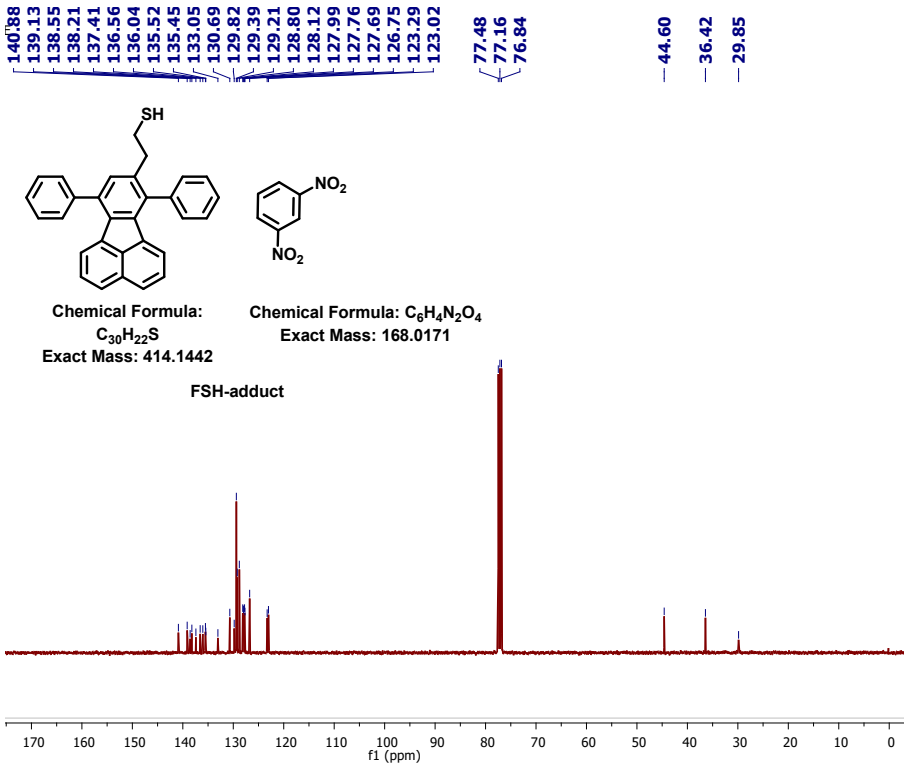

Fig. S11 ^{13}C NMR (100 MHz) spectrum of compound FSH-adduct in $CDCl_3$.

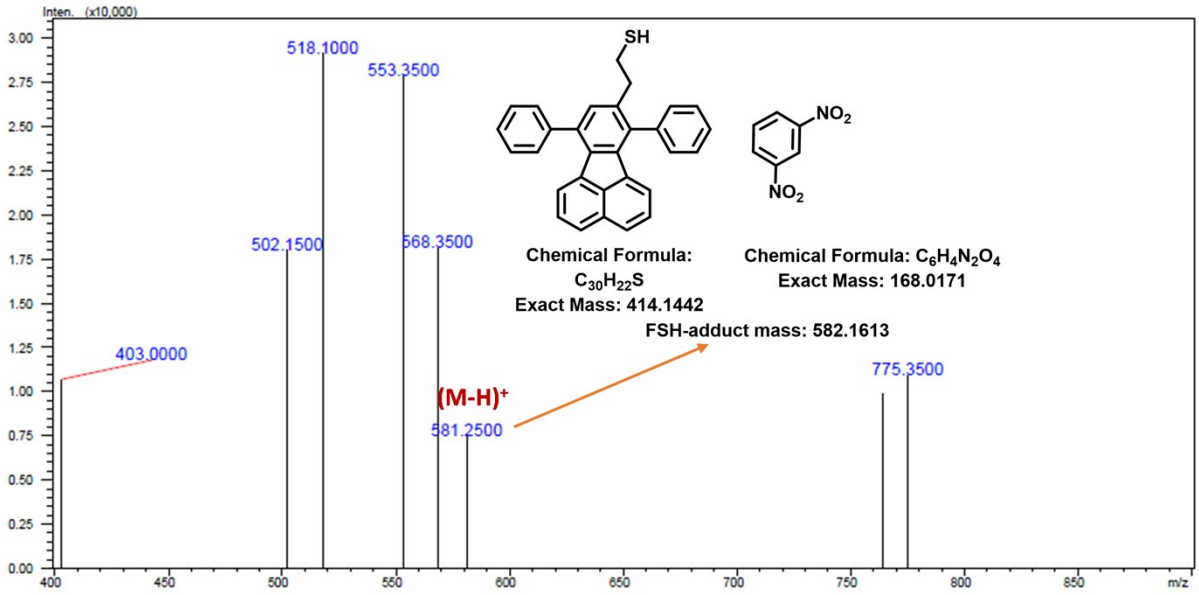

Fig. S12 ESI-MS spectrum of compound FSH-adduct.

8. FT-IR of FOH, FSH and FSH-adduct

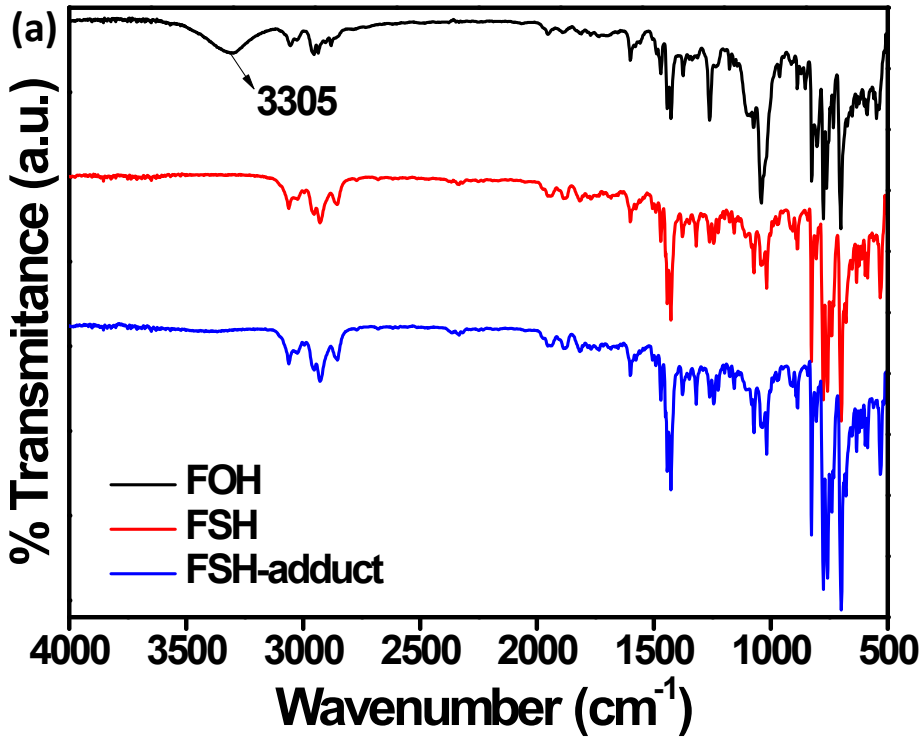

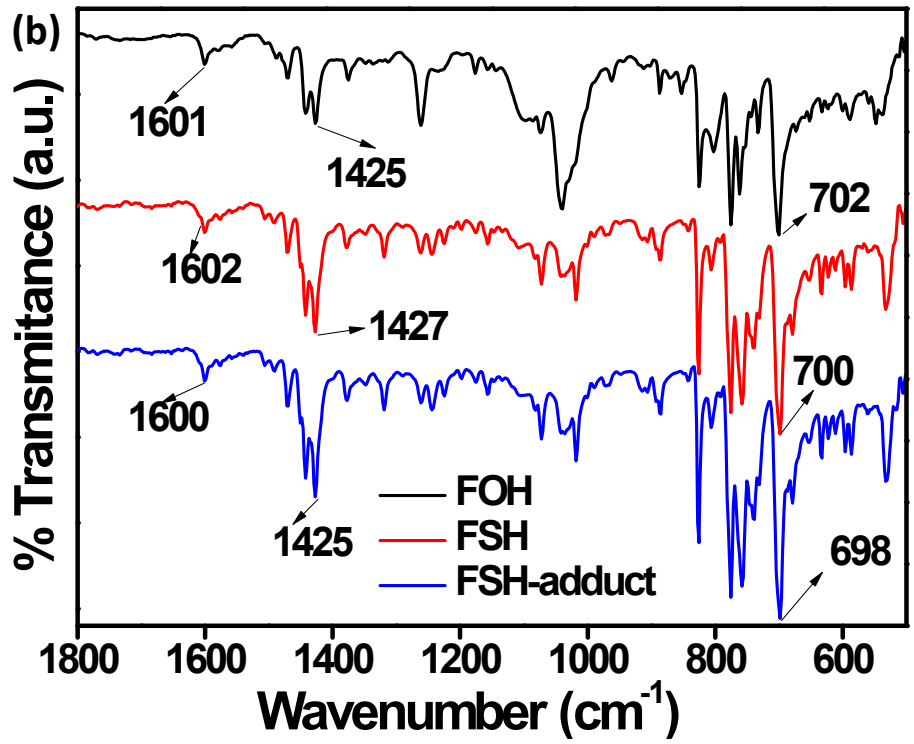

Fig. S13 FT-IR spectra of compound FOH, FSH and FSH-adduct wavelength range from 4500-500 cm^{-1} (a) and 1800-500 cm^{-1} (b).

9. DSC

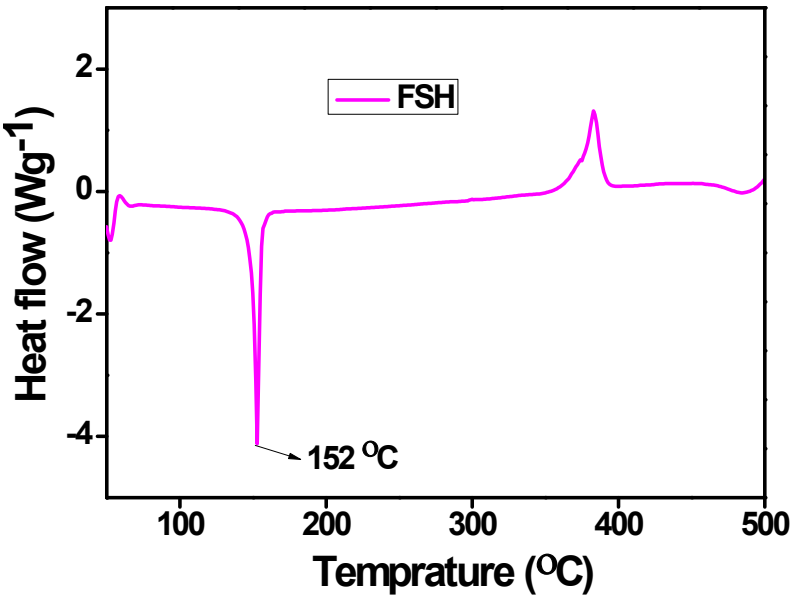

Fig. S14 DSC thermograms of FSH under the nitrogen flow with heating rate of 5°C/min.

10. Single crystal X-ray diffraction

Single crystals for x-ray diffraction were grown from chloroform with few drops of methanol with the slow solvent evaporation method. Single crystal X-ray data of FOH and FSH were collected using a Rigaku Oxford Diffraction XtaLAB Synergy-S diffractometer equipped

with a HyPix-6000HE Hybrid Photon Counting (HPC) detector and Cu microfocus sealed X-ray tube, as well as a low-temperature Oxford Cryosystems Cobra low temperature device. The data collection strategy was calculated within CrysAlisP (Rigaku OD, 2021; Table S1) to ensure desired data redundancy and percent completeness. The Structure is solved using SHELXT(Sheldrick, 2015b)[2] and refined by least-squares refinement on F^2 followed by difference Fourier synthesis (OLEX2, SHELXL) (Dolomanov et al., 2009; Sheldrick, 2015a)[3,4]. The space group determination was performed by using PLATON(Spek, 2009)[5]. All non-hydrogen atom positions were located using difference Fourier methods and refined anisotropically. Hydrogen atom positions were calculated using the HFIX command and constrained during the refinement. Additional details of the data collection and structural refinement parameters are provided in Supplementary Table 1.

Single crystal X-ray diffraction data of FSH-adduct was collected on an Oxford Xcalibur Mova E diffractometer equipped with an EOS CCD detector and a micro focus sealed tube using Mo Kα radiation (λ = 0.71073 Å) using an Oxford Cobra open stream non-liquid nitrogen cooling device. Crystal data collection and reduction were performed using CrysAlisPro (version 1.171.38.46).[2] The Structure is solved using SHELXT(Sheldrick, 2015b)[2] and refined by least-squares refinement on F^2 followed by difference Fourier synthesis (OLEX2, SHELXL) (Dolomanov et al., 2009; Sheldrick, 2015a)[3,4]. All non-hydrogen atoms were refined anisotropically and hydrogen atoms on heteroatoms were located from difference electron density maps and all C-H atoms were fixed geometrically using HFIX command. Packing diagrams were generated by using MERCURY.[6] ORTEP diagrams were generated using ORTEP-3.[7]

Table 1 Crystal data and structure refinement for FOH, FSH and FSH-adduct

Identification code	**FOH**	**FSH**	**FSH.DNB**
CCDC No.	2179068	2178647	2231960
Empirical formula	$C_{30}H_{22}O$	$C_{30}H_{22}S$	$C_{36}H_{26}N_2O_4S$
Formula weight	398.47	414.53	582.65
Temperature/K	293(2)	169.8(5)	100.02(11)
Crystal system	monoclinic	monoclinic	monoclinic
Space group	$P2_1/n$	$P2_1/c$	$P2_1/c$
a/Å	11.17078(8)	28.3784(2)	6.7392(3)
b/Å	20.07704(13)	9.76550(10)	16.2759(5)
c/Å	19.46098(14)	23.8510(2)	25.2215(9)
α/°	90	90	90
β/°	97.9360(7)	93.1820(10)	92.282(3)
γ/°	90	90	90
Volume/Å^3	4322.83(5)	6599.62(10)	2764.27(18)
Z	8	12	4
ρ_{calc}g/cm^3	1.225	1.252	1.400
μ/mm^{-1}	0.558	1.397	0.164
F(000)	1680.0	2616.0	1216.0
Crystal size/mm^3	0.16 × 0.124 × 0.065	0.16 × 0.124 × 0.065	0.125 × 0.014 × 0.01
Radiation	Cu Kα (λ = 1.54184)	CuKα (λ = 1.54184)	MoKα (λ = 0.71073)
2Θ range for data collection/°	6.356 to 153.82	7.424 to 153.634	6.466 to 54.968
Index ranges	-14 ≤ h ≤ 12, -24 ≤ k ≤ 14, -24 ≤ l ≤ 22	-35 ≤ h ≤ 21, -12 ≤ k ≤ 12, -30 ≤ l ≤ 30	-8 ≤ h ≤ 8, -20 ≤ k ≤ 21, -32 ≤ l ≤ 32
Reflections collected	31863	51270	37382
Independent reflections	8808 [R_{int} = 0.0218, R_{sigma} = 0.0195]	13356 [R_{int} = 0.0347, R_{sigma} = 0.0323]	6297 [R_{int} = 0.0733, R_{sigma} = 0.0580]
Data/restraints/parameters	8808/0/562	13356/0/841	6297/0/389
Goodness-of-fit on F^2	1.023	1.036	1.047
Final R indexes [I>=2σ (I)]	R_1 = 0.0413, wR_2 = 0.1136	R_1 = 0.0434, wR_2 = 0.1144	R_1 = 0.0738, wR_2 = 0.1464
Final R indexes [all data]	R_1 = 0.0460, wR_2 = 0.1177	R_1 = 0.0543, wR_2 = 0.1218	R_1 = 0.0996, wR_2 = 0.1599
Largest diff. peak/hole / e Å^{-3}	0.21/-0.19	0.40/-0.50	1.04/-0.55

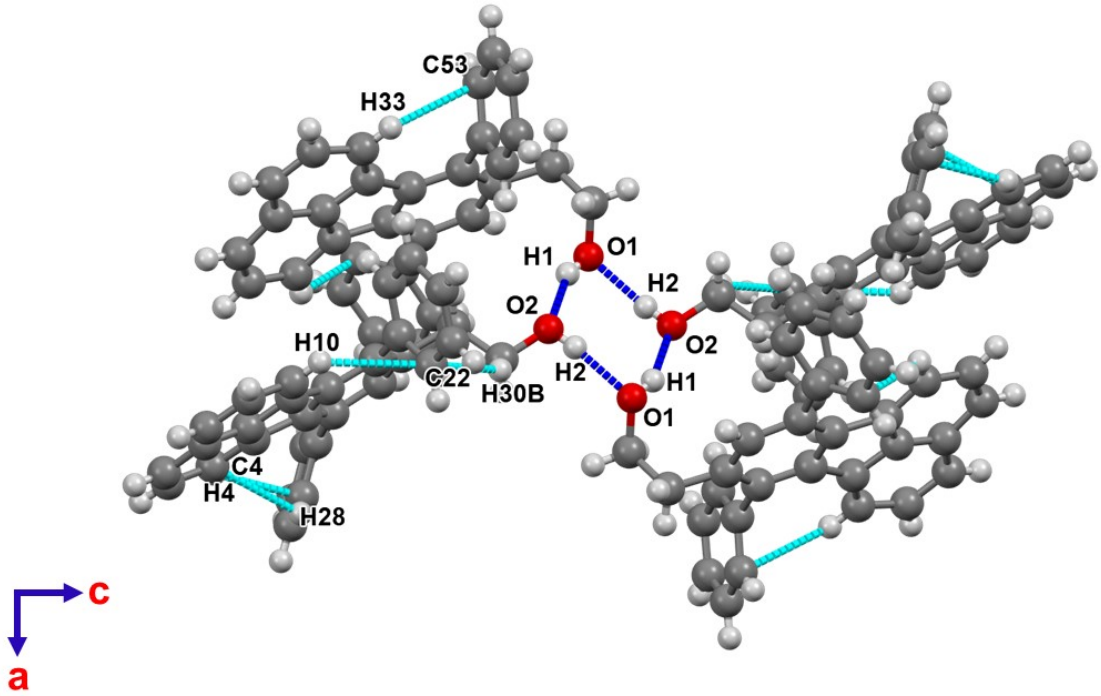
C53
H33
H1
O1
H2
O2
O2
H10
C22
H30B
H2
H1
O1
C4
H4
H28
c
a

(a)

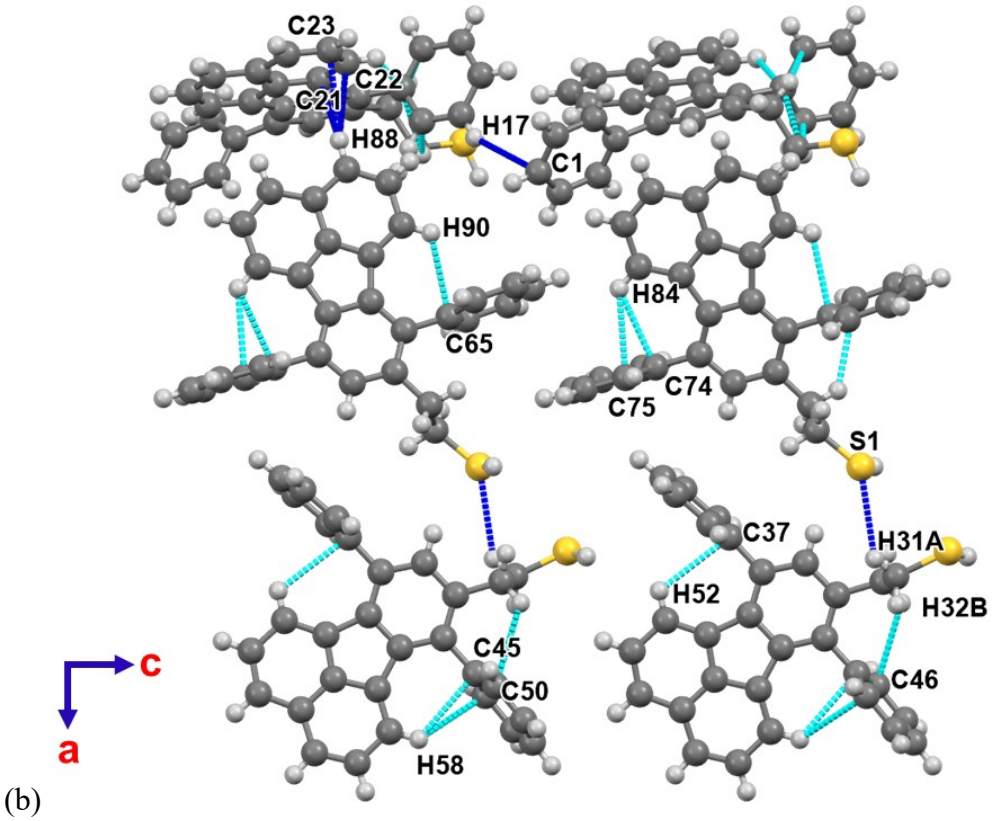
C23
C22
C21
H88
H17
C1
H90
C65
H84
C74
C75
S1
C37
H31A
H52
H32B
C45
C50
C46
H58
c
a

(b)

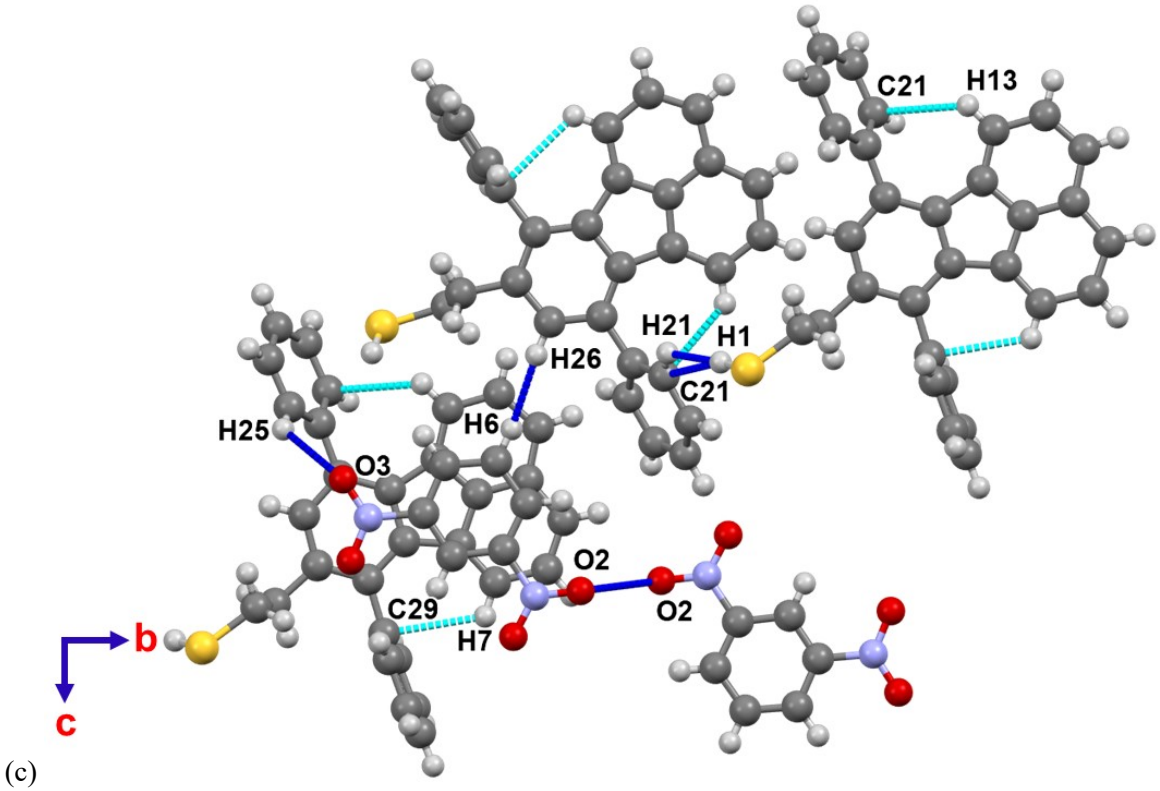

(c)

Fig. S15. Inter (blue) and intra (cyan) molecular hydrogen bonding interaction of (a) FOH (b) FSH and (c) FSH.DNB adduct.

11. Optical bandgap (UV-Vis) Tauc plot of FOH and FSH in THF and in thin film

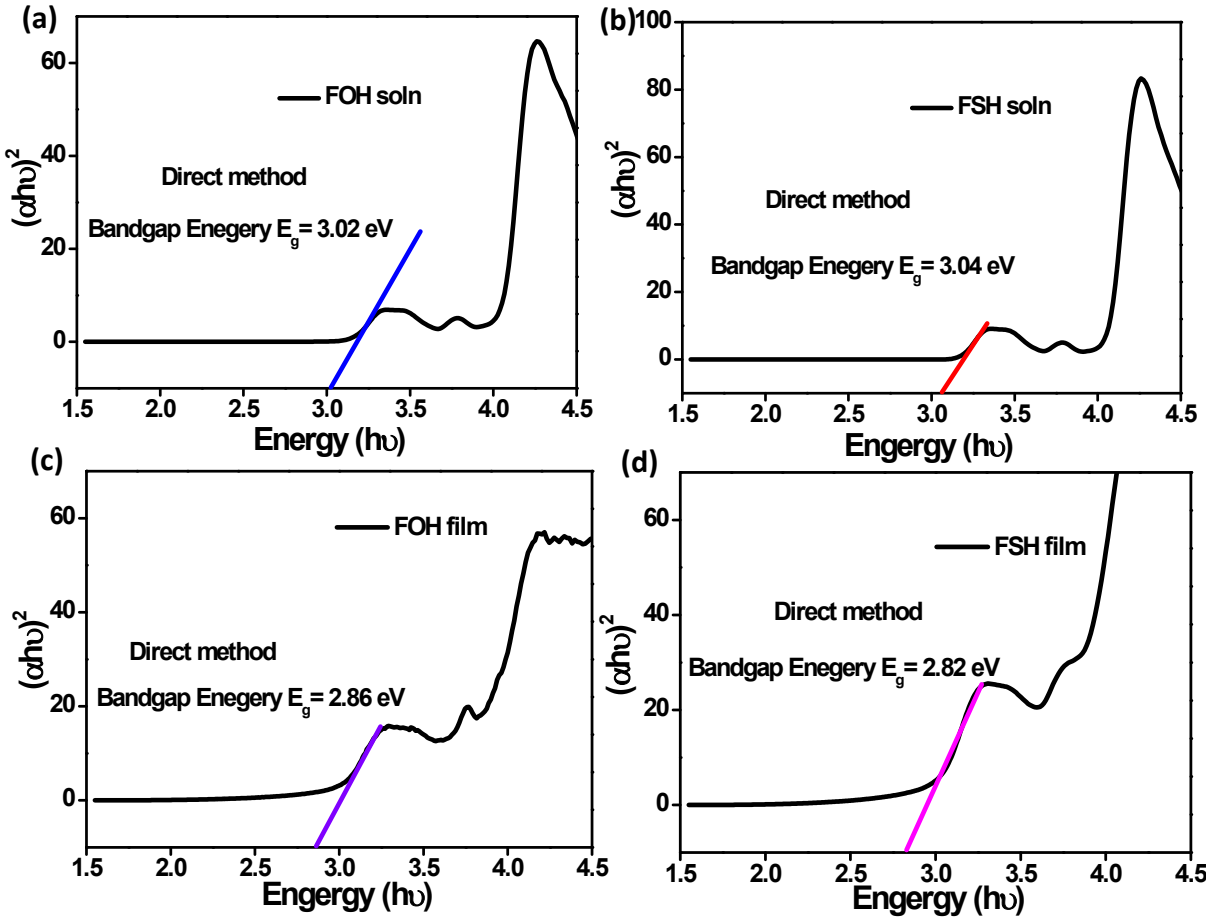

Fig. S16 Optical bandgap (Tauc's plot) of FOH and FSH in THF and in thin film

12.1. Fluorescence studies

The FSH and FOH stock solution were made by dissolving it in THF at a concentration of 1 x 10^{-3} M. The stock solutions of nitro analyte were prepared by dissolving the them in methanol with a concentration of 1 x 10^{-3} M. The emission spectra of the fluorophore were examined by adding a 2 µL of a stock solution of respective flurophore in 2 mL of THF solution. Further, the effective NACs on fluorescence intensity was investigated by adding a few microliters of a stock solution of the nitro analytes. To get a stable fluorescence signal, the solution was then given a few minutes to equilibrate. The formula $(I_0\text{-}I)/I_0$ x 100% was used to calculate the quenching efficiency (%), where I_0 and I are the fluorescence intensity in the system before and after addition of an analyte, respectively.

12.2. Fluorescence lifetime and Quantum yield studies

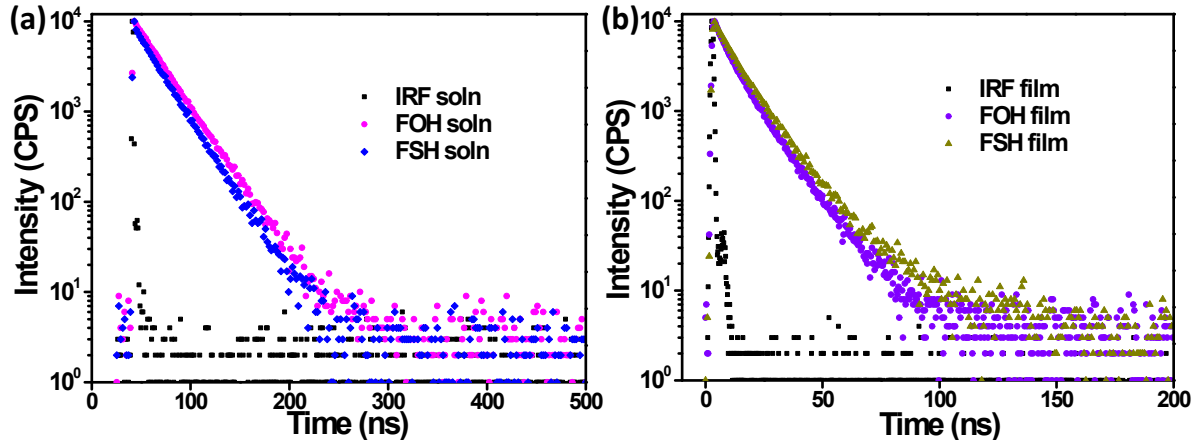

Fig. S17 Fluorescence lifetime decay of FOH and FSH in (a) THF and (b) thin film.

Table S2 Summary of FOH and FSH fluorescence lifetime measurement and quantum yield

Code	Lifetime in ns,		Quantum yield Φ (%) (solution)
	Solution (Relative amplitude, %)	Thin film (Average Lifetime)	
FOH	26 (100)	10.55	29.96
FSH	24 (100)	12.81	60.69

13. Chemosensing behaviour FSH with different NACs

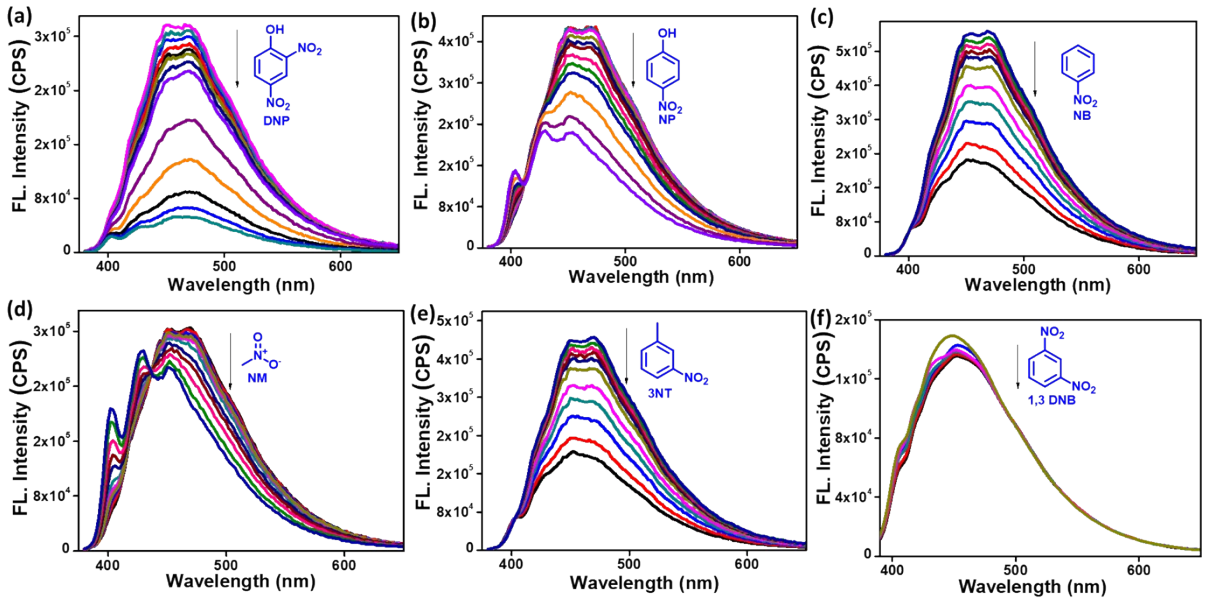

Fig. S18 (a-f) Change in the emission intensity of FSH (1 μM) upon addition of different concentrations (0-1000 μM) of various nitro compounds.

14. Chemosensing behavior FOH with different NACs

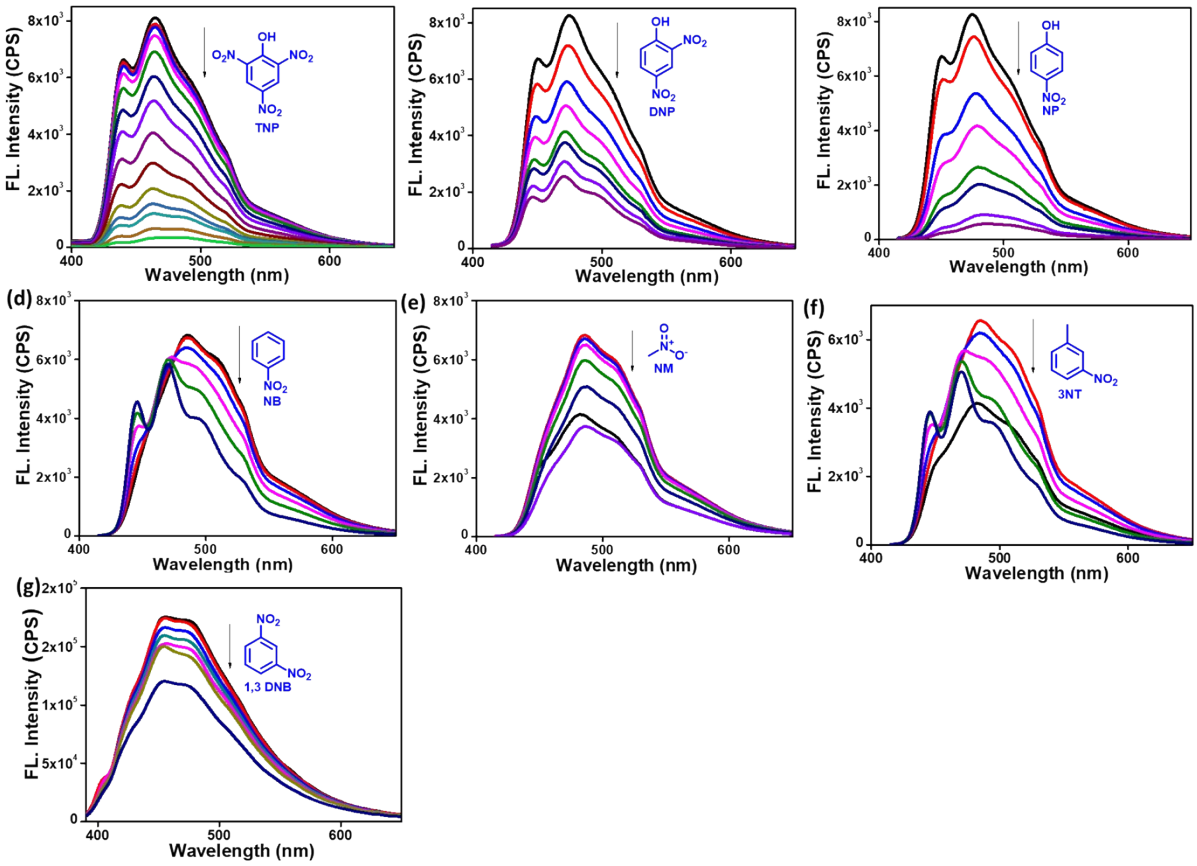

Fig. S19 (a-g) Change in the emission intensity of FOH (1 μM) upon addition of different concentrations (0-1000 μM) of various nitro compounds.

15. Stern-Volmer rate constants

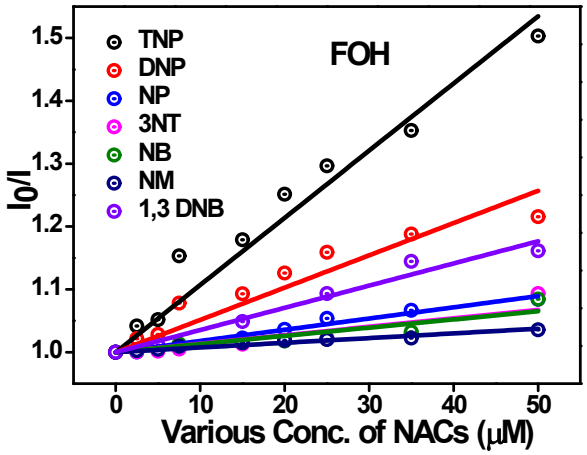

Fig. S20 Stern-Volmer plot of FOH (1 μM) treated with various concentrations of NACs (50 μM).

Table S3 Summary of the Stern-Volmer rate constants (K_{SV}) of FSH and FOH treated with various nitro derivatives in THF.

Analyte	FSH (M^{-1})	FOH (M^{-1})
TNP	0.0111	0.01069
DNP	0.0055	0.00514
NP	0.0013	0.0017
3NT	0.00104	0.00135
NB	0.0011	0.0013
NM	0.0007	0.0007
1,3 DNB	0.00313	0.00353

16. LOD's of FSH with TNP

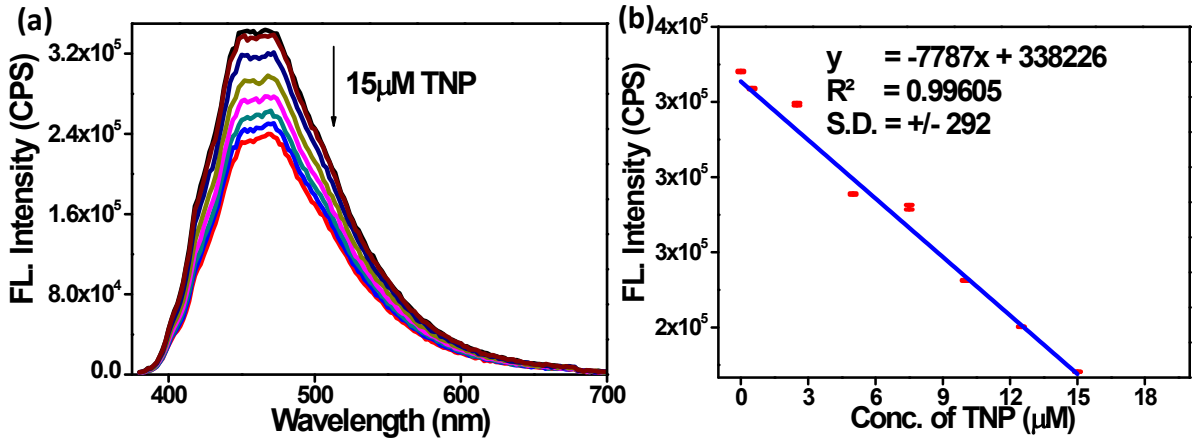

Fig. S21 (a) Change in the emission spectra of FSH (1 μM) in THF upon the addition of different concentrations of TNP (15 μM). (b) Change in the emission intensity at ~ 450 nm for different concentrations of TNP. The reproducibility of the data was tested for three independent experiments to determine the error analysis. In most cases, dispersion of error is found between ± 292 and the data was represented with an average standard deviation.

Table S4 Summary on LOD of FSH treated with TNP and real samples

Code	TNP	TNP (River water)
FSH	**97 ppm**	**76 ppm**

17. Fluorescence lifetime titration data of FSH with different concentration of TNP

Table 5 Summary on lifetime information of FSH with different concentration of TNP

Code	Lifetime in ns, (Relative amplitude, %)
FSH	**15 (100)**
FSH + 50 µM of TNP	**14.5 (100)**
FSH + 250 µM of TNP	**14.4 (100)**
FSH + 500 µM of TNP	**13 (100)**
FSH + 1000 µM of TNP	**9.6 (100)**

18. Spectrophotometric titration of fluoranthene derivatives with TNP

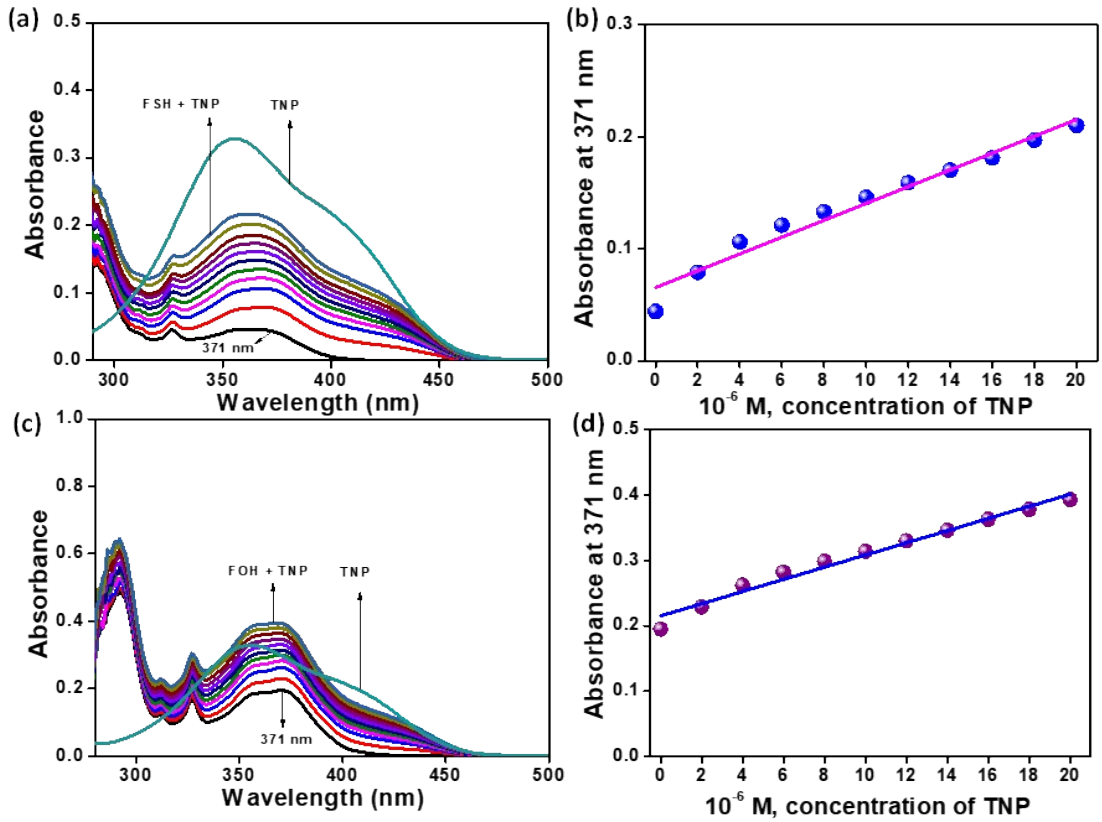

Fig. S22. (a-b) UV-Vis titration spectra and isotherm of FSH (20 µM) upon the addition of TNP (0-20 µM) in THF respectively. (c-d) UV-Vis titration spectra and isotherm of FOH (20 µM) upon the addition of TNP (0-20 µM) in THF respectively

19. Analysis of FSH toward TNP in real samples

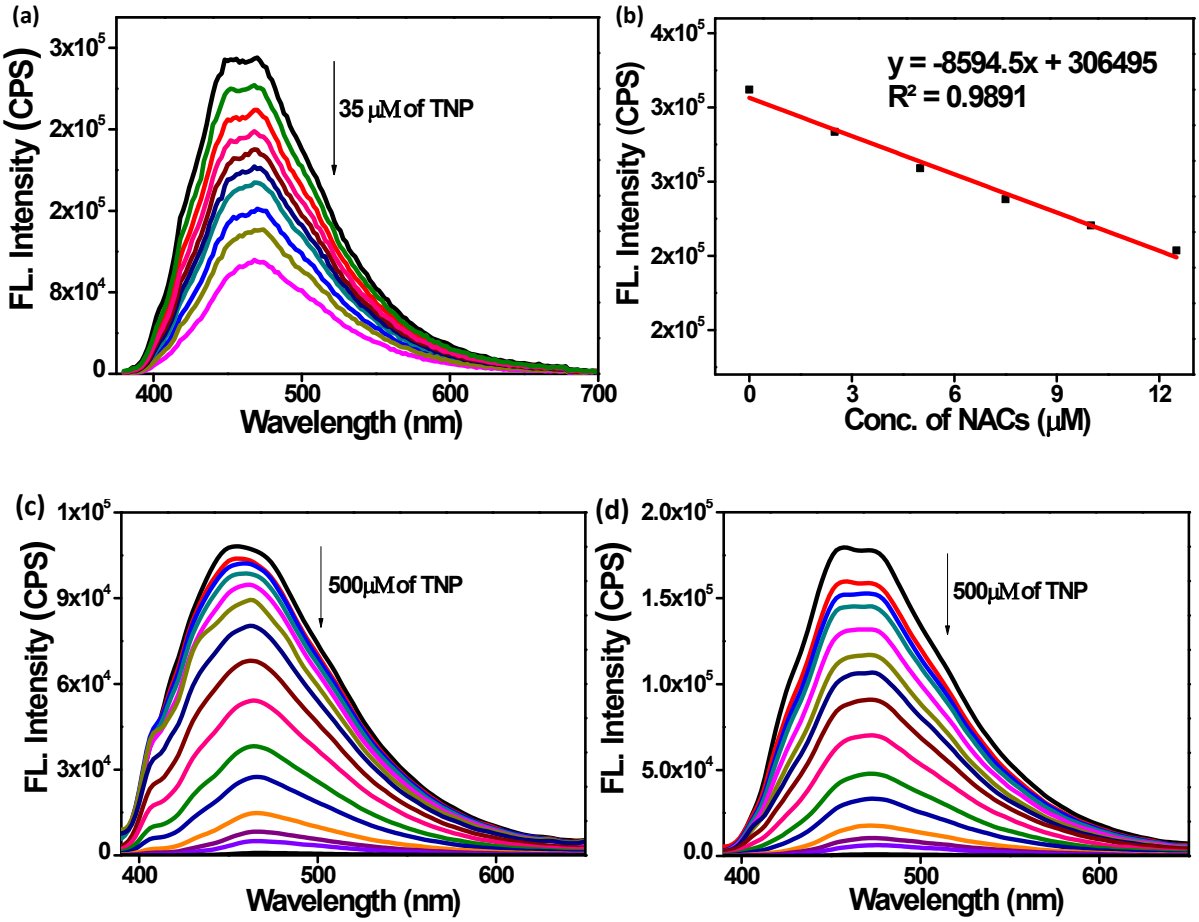

Fig. S23 (a) Change in the emission spectra of FSH (1 μM) in THF upon the addition of different concentrations of spiked TNP (35 μM) in real time analysis. (b) Change in the emission intensity at ~ 450 nm for different concentrations of spiked TNP in real time analysis. Change in the emission behaviour of 1μM concentration of (c) FSH and (d) FOH with various concentration of TNP (up to 500 μM) in THF:H_2O (1:1 v/v) mixture.

Table S6 Result for the determination of TNP in the real samples

River samples	TNP spiked	TNP found	Recovery (%)
1	0.1	0.076	76
2	0.2	0.161	80
3	0.3	0.238	79

20. Analysis of FSH and FOH with Toluene and Xylene

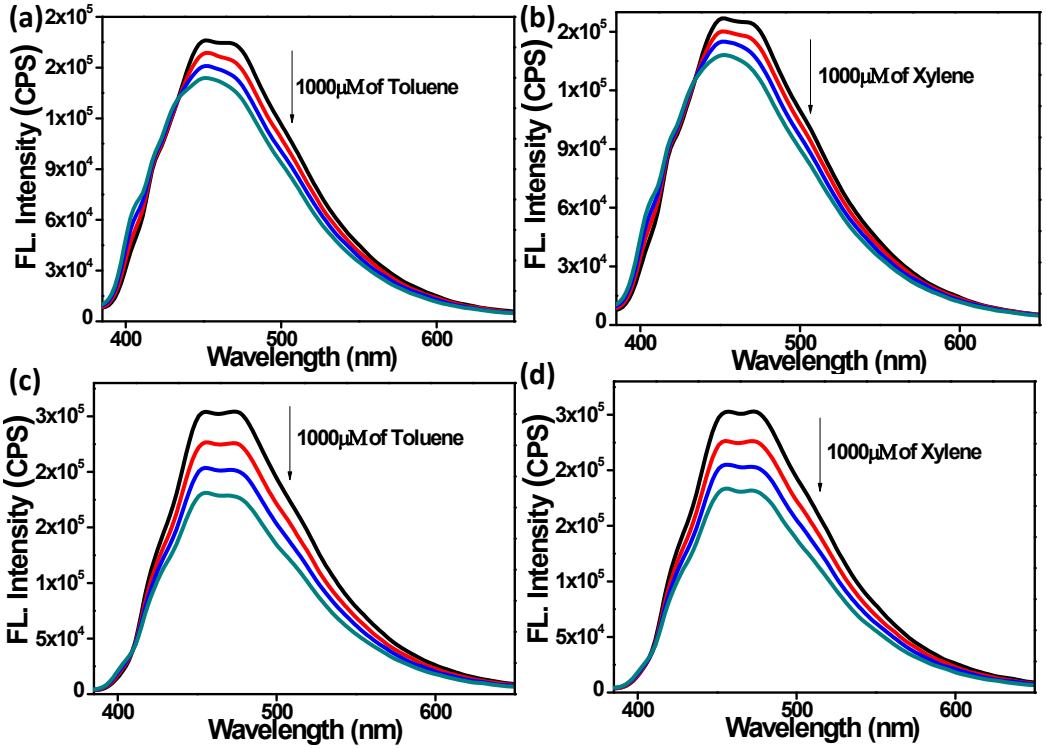

Fig. S24 Change in the emission intensity of FSH (1 μM) upon addition of different concentrations (0-1000 μM) of (a) Toluene and (b) Xylene. Change in the emission intensity of FOH (1 μM) upon addition of different concentrations (0-1000 μM) of (c) Toluene and (d) Xylene.

21. Interference study of FSH and FOH with TNP in presence of metal ions

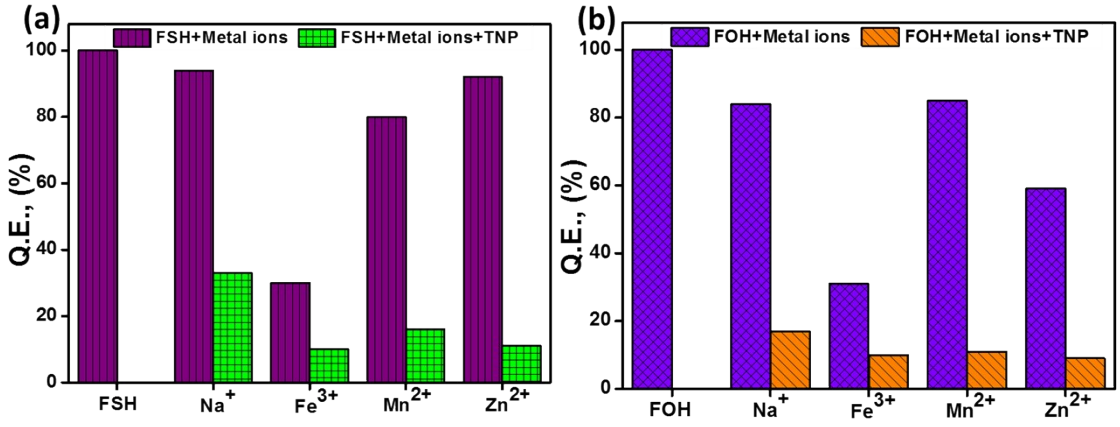

Fig. S25 (a) Interference study of FSH (1 μM) with TNP (500 μM) in presence of other metal analytes (500 μM) (b) Interference study of FOH (2 μM) with TNP (500 μM) in presence of other metal analytes (500 μM).

22. Studies with Zebrafish

In order to assess the developmental toxicity of FOH, FSH, and TNP zebrafish embryos were tested following OECD Fish embryo toxicity guidelines for a period of 96 hours.[8] A range of concentrations like 10, 20, 40, 60, 80, and 100 µg/ml were used to find the median lethal concentration. Following that, hatching rate of zebrafish embryos were also assessed from 48 h onwards till 96 hours. In a separate set of experiment, 72 hpf zebrafish larvae was used to assess the fluorescence emitted by FSH, FOH and their quenching by TNP. The lowest tested concentration 10 µg/ml was chosen to study fluorescence activity on live zebrafish larvae. The fluorescence images were captured using Nikon Eclipse Ti2, New York, USA along with their respective control images and analyzed through Image J software.

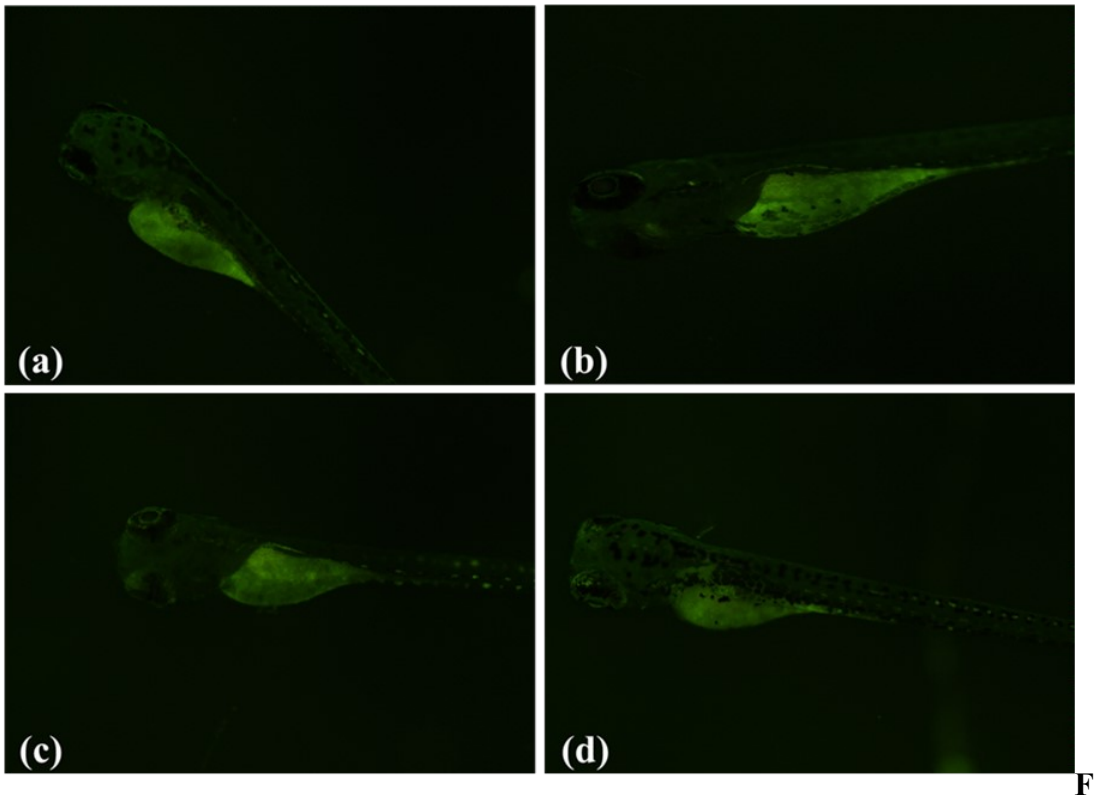

Fig. S26 FOH florescence quantification on 72hpf zebrafish larvae (a) Water control (b) DMSO (c) FOH (d) FOH + TNP.

22.1 Acute behavioral toxicity Testing

Acute behavioral toxicity of FSH and FOH on adult zebrafish with a concentration of 10mg/L, to assess the swimming behavior and other different behavioral end points as suggested by Kalueff et al.[9] A small glass aquariums filled with 1 L of water was used to assess the behavior.

One fish was used at a time both in control and in treated and the experiment was repeated thrice and behavioral end points were recorded Fig S27-28.

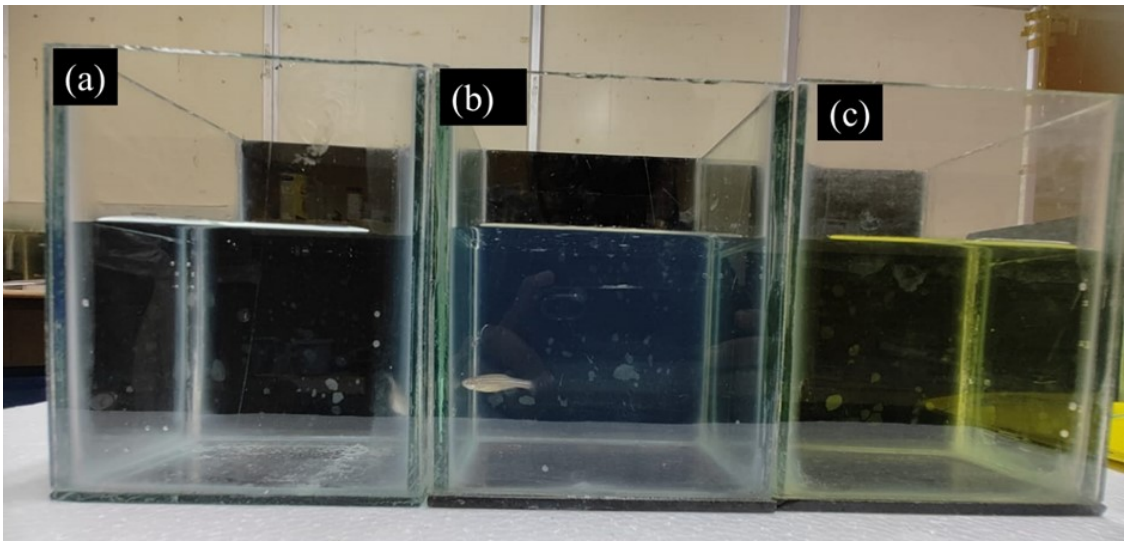

Fig. S27 Acute behavioral toxicity of FSH on zebrafish. (a) DMSO solvent control (b) FSH (c) TNP.

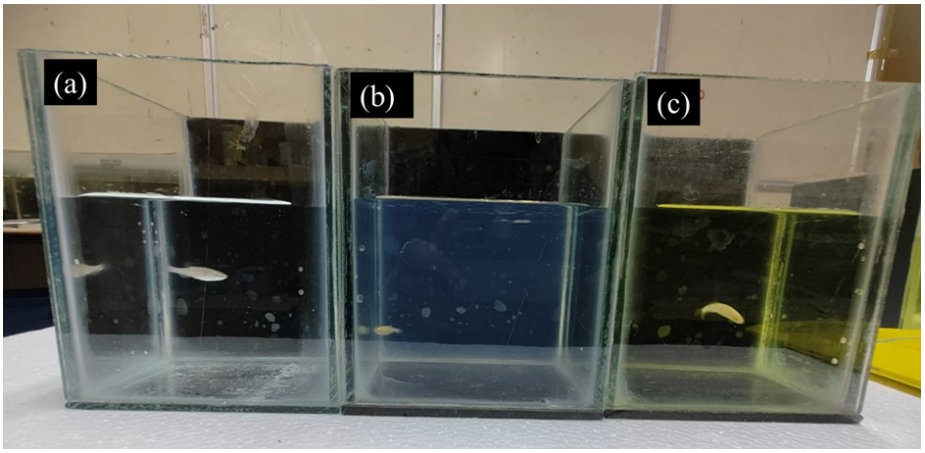

Fig. S28 Acute behavioral toxicity of FOH on zebrafish. (a) DMSO solvent control (b) FOH (c) TNP.

23. References

1. K. Selvaraj, P. B. Managutti, S. Mohamed, S. Talam, V. Nutalapati, Importance of the donor unit on fluoranthene for selective detection of nitro aromatic explosives, *Journal of Photochemistry and Photobiology A: Chemistry*, 2022, **433**, 114215.

2. G. M. Sheldrick, SHELXT - Integrated Space-Group and Crystal-Structure Determination, *Acta Crystallographica Section A: Foundations of Crystallography*, 2015, **71**, 3-8.

3. O. V, Dolomanov, L. J. Bourhis, R. J. Gildea, J. A. K. Howard, H. Puschmann, OLEX2: A Complete Structure Solution, Refinement and Analysis Program, *Journal of Applied Crystallography*, 2009, **42**, 339-341.

4. G. M. Sheldrick, Crystal Structure Refinement with SHELXL, *Acta Crystallographica Section C: Structural Chemistry*, 2015, **71**, 3-8.

5. A. L. Spek, Structure Validation in Chemical Crystallography, *Acta Crystallographica Section D: Biological Crystallography*, 2009, **65**, 148-155.

6. C. F. Macrae, I. Sovago, S. J. Cottrell, P. T. A. Galek, P. McCabe, E. Pidcock, M. Platings, G.P. Shields, J. S. Stevens, M. Towlera and Peter A. Wood, *J. Appl. Cryst.,* 2020, **53**, 226.

7. Farrugia, L. J. ORTEP -3 for Windows - a version of ORTEP -III with a Graphical User Interface. (GUI). *J. Appl. Crystallogr*. 1997, **30**, 565–565.

8. OECD, OECD TG 236 test guidelines for testing of chemicals. Fish embryos acute toxicity (FET) tests, 2013, 1-22.

9. A.V. Kalueff, M. Gebhardt, A. M. Stewart, J. M. Cachat, M. Brimmer, J. S. Chawla, C. Craddock, E. J. Kyzar, A. Roth, S. Landsman, S. Gaikwad, K. Robinson, E. Baatrup, K. Tierney, A. Shamchuk, W. Norton, N. Miller, T. Nicolson, O. Braubach, C. P. Gilman, J. Pittman, D. B. Rosemberg, R. Gerlai, D. Echevarria, E. Lamb, S. C. Neuhauss, W. Weng, L. Bally-Cuif, H. Schneider, Zebrafish Neuroscience Research Consortium, Towards a comprehensive catalog of zebrafish behavior 1.0 and beyond, *Zebrafish*, 2013, **1**, 70-86.